# Gravitational Lensing Statistics in a Flat Universe

Myeong-Gu Park
*Department of Astronomy and Atmospheric Sciences,*
*Kyungpook National University, Taegu 702-701, Korea*

*to appear in the Journal of Korean Physical Society*



## Abstract

The probability distribution of lens image separations is calculated for the "standard" gravitational lensing statistics model in an arbitrary, flat Robertson-Walker universe, where lensing galaxies are singular isothermal spheres that follow the Schechter luminosity function. In a flat universe, the probability distribution is independent of the source distribution in space and in brightness. The distribution is compared with observed multiple-image lens cases through Monte-Carlo simulations and the Kolmogorov-Smirnov test. The predicted distribution depends on the shape of the angular selection bias used, which varies for different observations. The test result also depends on which lens systems are included in the samples. We mainly include the lens systems where a single galaxy is responsible for lensing. We find that the "standard" model predicts a distribution which is different from the observed one. However, the statistical significance of the discrepancy is not large enough to invalidate the "standard" model with high confidence. Only the radio data reject the model at the 95% confidence level, which is based on four/three lens cases. Therefore, we cannot say that the observational data reject the "standard" model with enough statistical confidence. However, if we take the velocity dispersion of dark matter without the conversion factor $(3/2)^{1/2}$ from that of luminous matter, the discrepancy is quite severe, and even the ground-based optical survey data reject the "standard" model with $\gtrsim 90\%$ confidence.

PACS numbers: 95.30.S, 98.62.S, 98.54.Aj, 98.65.Dx, 98.80.Es

## I. INTRODUCTION

Determining the geometry of the universe and the distributions of masses therein has always been one of the most important goals of astronomy. Even before the actual discovery of gravitational lenses, it was known that lens systems could provide us much useful information on these fundamental questions [3].

As more high-redshift multiply imaged QSOs were discovered, Turner et al. [1] calculated the statistical properties of multiple-image gravitational lenses in the standard Robertson-Walker cosmology, especially the probability of a QSO being multiply imaged and the mean angular separation of images [1]. They compared the predicted statistical properties of the lens systems with observations and concluded that although more small-separation ($\lesssim 1''$) lenses are expected, the distribution of the image separation, with the effect of resolution bias considered, is compatible with the observed lens systems. Gott et al. extended this work to an arbitrary Robertson-Walker universe [4]. The probability of lensing and the mean image separation were expressed as functions of the source redshift. However, the explicit value of the mean image separation was not calculated, and only the functional form was compared with the data to get the limits on the cosmological parameters. One interesting fact recognized in this work, and partly in Ref. [1], is that in a flat universe filled with singular isothermal sphere (SIS) galaxies, the mean separation of images is independent of the source distance (or redshift), regardless of the value of the dimensionless cosmological constant, $\lambda_0 \equiv \Lambda/3H_0^2$ where $H_0$ is the Hubble constant.

Turner [5] and Fukugita et al. [6] subsequently realized that the probability of lensing, rather than the image separation, is more sensitive to $\lambda_0$. In a series of papers [7,8], they estimated how many multiple-image lens systems should be discovered for given QSO samples in a $\lambda_0$-dominated universe and found the present number of observed lens systems exclude $\lambda_0 \gtrsim 0.9$. This limit is considered as one of the few observational limits on the elusive cosmological constant.

However, if we naively use the various galaxy parameters of Ref. [8] to recalculate the expected mean separation in a flat universe following Ref. [4], we get $1.5''$. This is significantly smaller than the observed image separations in known single-galaxy lens systems (systems in which a single galaxy is responsible for lensing), e.g., PG1115, Q2237, Q0142, H1413, MG0414, and B1422 (Table I) whose mean value is $1.95''$and whose dispersion $0.70''$. If we take the most favorable galaxy parameters allowed within the uncertainty interval in Ref. [7], the mean separation goes up to $1.7''$, still somewhat small compared to the observed image separations. However, the angular resolution bias, larger splitting lens systems being easier to find, which was not considered in Ref. [4] and which was minimally incorporated in Refs. [7] and [8] might change this interesting discrepancy. Also, a better statistical test is needed because of the non-standard shape of the distribution and the small sample size.

The usual criticism against utilizing image separation data has been its dependence on a combination of cosmological parameters [4]. However, this can be an advantage if we want to test the curvature of the universe or the consistency of the lensing statistics model without being affected by the uncertainties in the cosmological parameters. Moreover, the distribution of the image separations is relatively independent of the magnification bias which introduces major uncertainty when the probability of lensing is used as a cosmological diagnostic tool.

In this work, we adopt the same assumptions and parameters for galaxies as in Ref. [7] to get the probability distribution of the image separations, incorporating all possible angular resolution biases present in various lens surveys. By comparing this distribution with observed single-galaxy lens data (Table 1), we test the "standard" gravitational lensing statistics model against the observations. We choose a flat universe with arbitrary $\lambda_0$ as the background universe.

## II. PROBABILITY DISTRIBUTION OF IMAGE SEPARATION

A flat universe with a non-zero cosmological constant can be described by the Robertson-Walker metric [4]

$$ds^2 = -c^2dt^2 + \frac{a^2(t)}{a_0^2}[a_0^2 d\chi^2 + a_0^2\chi^2(d\theta^2 + \sin^2\theta d\phi^2)]. \tag{1}$$

The expansion factor $a(t)$ has as its present value $a_0 = R_0/\Delta$, where $R_0 \equiv c/H_0$ and $\Delta = (|\Omega_0 + \lambda_0 - 1|)^{1/2}$ if the value inside the square-root is not zero and $\Delta = 1$ if it is zero. Among several relevant cosmological distances, we use the parametric distance $\chi$, which is equivalent to the (filled-beam) standard angular distance (see Ref. [8]).

Galaxies are modeled as SIS; therefore, their lensing properties are determined by a one-dimensional velocity dispersion, $\sigma$, which is related to the galaxy luminosity by $L/L^* = (\sigma/\sigma^*)^\gamma$ where $\gamma = 4$ for E and SO galaxies and $\gamma = 2$ for for S galaxies [9,7]. The luminosities of the galaxies follow the Schechter function

$$\Phi(L)dL = \Phi^* \left(\frac{L}{L^*}\right)^{\alpha_g} \exp(-L/L^*)\frac{dL}{L^*} \tag{2}$$

where $\alpha_g = -1.1$ [10]. The exact values of the typical luminosity of a galaxy, $L^*$, and its normalization constant, $\Phi^*$, are important in lensing probability estimates, but are irrelevant in this work because only the functional shape of the distribution matters. If there are galaxy evolutions, $\Phi^*$ and $L^*$ become functions of $\chi$ (or redshift).

Under these assumptions, the lensing probability by one type of galaxy is simply given as [4]

$$d^2\tau = \pi a_0^3(\alpha^*)^2\Phi^* \left(\frac{L}{L^*}\right)^{\alpha_g+4/\gamma} e^{-L/L^*}\left[\frac{(\chi_S-\chi_L)^2\chi^2}{\chi_S^2}\right] d\left(\frac{L}{L^*}\right) d\chi_L \tag{3}$$

where $\chi_S$ and $\chi_L$ are the parametric distance to the source and the lens, respectively, and $\alpha^* \equiv 4\pi(\sigma^*/c)^2$, the bending angle for an $L^*$ galaxy. Since the image separation $\Delta\theta = 2\alpha^*(L/L^*)^{2/\gamma}(\chi_S - \chi_L)/\chi_S$, the probability can be rewritten as a function of $\Delta\theta$ or $\varphi \equiv \Delta\theta/(2\alpha^*)$:

$$\begin{aligned} d^2\tau = {} & \frac{\pi}{2}\gamma a_0^3(\alpha^*)^2\Phi^*\varphi^{(\alpha_g+1)\gamma/2+1} \exp\left[-(\frac{\chi_S-\chi_L}{\chi_S})^{-\gamma/2}\varphi^{\gamma/2}\right] \\ & \times \frac{(\chi_S-\chi_L)^2\chi_L^2}{\chi_S^2}\left[\frac{\chi_S-\chi_L}{\chi_S}\right]^{-\gamma(\alpha_g+1+4/\gamma)/2} d\varphi d\chi_L. \end{aligned} \tag{4}$$

The total probability of lensing by all types of galaxies is

$$\tau = \sum_{i=\mathrm{E,S0,S}} \int_0^\infty d\varphi_i \int_0^{\chi_S} d\chi_L \frac{d^2\tau_i}{d\varphi_i d\chi_L} \tag{5}$$

where $d\tau_i$ and the other symbols with subscript $i$ refer to the respective values for E, S0, and S galaxies.

All lens observations and surveys suffer from some kind of angular selection bias mainly due to the finite angular resolution. If this bias is taken account, the probability distribution function (PDF) of observed image separations becomes

$$\frac{dP}{d\Delta\theta} = \frac{1}{\tau}\int_0^{\chi_S} \sum_i \left(\frac{d^2\tau_i}{d\chi_L d\Delta\theta}\right) d\chi_L \tag{6}$$

$$= \frac{\sum_i (2\alpha_i^*)^{-1}\gamma_i F_i^* [\Gamma(\alpha_g + 1 + 4\gamma_i^{-1})]^{-1} \int_0^{\chi_S} d\chi_L G_i(\chi_L, \varphi_i)}{\sum_i \gamma_i F_i^* [\Gamma(\alpha_g + 1 + 4\gamma_i^{-1})]^{-1} \int_0^\infty d\varphi_i \int_0^{\chi_S} d\chi_L G_i(\chi_L, \varphi_i)} \tag{7}$$

with

$$G_i(\chi_L, \varphi_i) = f_s(\Delta\theta) \left[\frac{(\chi_S - \chi_L)\chi_L^2}{\chi_S}\right] \left[\frac{\chi_S}{\chi_S - \chi_L}\varphi_i\right]^{\gamma_i(\alpha_g+1)/2+1} \times \exp\left[-\Big(\frac{\chi_S}{\chi_S - \chi_L}\Big)^{\gamma_i/2} \varphi_i^{\gamma_i/2}\right] \tag{8}$$

where $\Gamma$ is the gamma function, $f_s(\Delta\theta)$ is a function describing the angular resolution bias with $\varphi_i = \Delta\theta/(2\alpha_i^*)$, and $F_i^* \equiv \pi\Phi_i^*(\alpha_i^*)^2 R_0^3 \Gamma(\alpha_g + 1 + 4\gamma_i^{-1})$ is the dimensionless parameter for the effectiveness of matter in producing double images for each type of galaxy [1,7]. We take the values for the various parameters from Ref. [8]. The cumulative distribution function (CDF)

$$P(\Delta\theta) = \int_0^{\Delta\theta} \left(\frac{dP}{d\Delta\theta'}\right) d\Delta\theta' \tag{9}$$

is calculated from $dP/d\Delta\theta$.

It can be proved with ease that in a flat universe the distribution is independent of $\chi_S$ (or $z_S$, the redshift of the source), regardless of the value of $\lambda_0$ or the functional form of the angular resolution bias [4]. This implies, regardless of the source distribution in space, any multiple-image lensing event should have the same image separation distribution as long as the universe is flat, which makes various statistical tests very simple. However, this is true only when there is no evolution in the lensing galaxies.

## III. OBSERVED MULTIPLE-IMAGE SYSTEMS AND ANGULAR SELECTION BIAS

The image separation is not affected by the absolute brightness of the sources as is the case with the lensing probability. However, it is affected by the finite angular resolution and by the dynamic range of the real observations; therefore, the angular selection bias

is a function of the image separation and the relative brightness of each image. Hence, to analyze statistically the distribution of image separations of lens systems discovered in specific surveys, one should carefully consider both effects as in Ref. [11]. However, since we approximate the lens by SIS in this work and since a given SIS lens produces always the same image separation regardless of the source position, the angular selection bias will be a function only of the image separation.

Since most of the lens cases are not discovered in one systematic survey and since each survey or observation is done under different conditions, a single universal function does not exist which can faithfully represent the angular selection effect in various different observations. Hence, we must use different specific angular selection biases for different observations. In this work, we consider four kinds of selection biases suitable for specific surveys: no selection bias (NO), the one for the HST snapshot survey [11,12] (HST), four similar selection biases appropriate for ground optical lens surveys [12] (PSF1.0, PSF0.7, EYE1.0, EYE0.7) one for a radio survey [15,2] (MG-C). Although the original forms for the selection biases HST, PSF1.0, PSF0.7, EYE1.0, and EYE0.7 depend on the brightness ratio of the images, we can disregard this dependence for the reasons explained above. Hence, we use Kochanek's completeness function [12] as the selection bias function because the image separation statistics are independent of the source brightness or the redshift distributions.

The lens samples and their corresponding selection biases with descriptions are listed in Table II and shown in Fig. 1: Inverted *big triangles*, *small triangles*, and *circles* denote the image separations of systems with a single galaxy lens or unknown lens, systems with a lens other than a single galaxy, and radio rings. We use only the accepted cases of multiple-image systems according to the criterion of Ref. [16]. Also, we basically exclude systems like 0957 (lensed by a galaxy and a cluster) and MG2016 (lensed by two galaxies) because we only consider single-galaxy lensing. However, the two systems are included in a special case for comparison. In systems like H1413 and MG0414, we do not know what kind of object is responsible for lensing. However, excluding those systems could introduce a bias against a small-separation system which has a less massive galaxy and, therefore, less chance of the lens being detected. For that reason, we include them as single-galaxy lens systems. Although system Q1208 is classified only as a proposed case in Ref. [16], it is meaningless to discuss the HST snapshot survey result without it [11], and we include it only for the HST survey. The test result regarding the HST survey should be taken with some cautions. Radio rings are included only in MG-C radio survey samples.

## IV. STATISTICAL TEST

Figure 1 shows the PDF's of the image separations for each angular selection bias. All of them peak around sub-arcsecond separations. However, all of the observed single-galaxy lens systems (*big triangles*) have image separations larger than $1''$, showing a discrepancy with theoretical expectations. To access the degree of discrepancy statistically, we use Monte-Carlo (MC) simulations [11] and the Kolmogorov-Smirnov (KS) test.

### A. Monte-Carlo Test

We define a likelihood function [11]

$$\ell \equiv \ln \left( \prod_{i=1}^{n} \frac{dP}{d\Delta\theta} |_{\Delta\theta_i} \right), \tag{10}$$

and generate $10^4$ sets of four to six random $\Delta\theta_i$'s following the calculated PDF and their respective $\ell$ values. These are compared with the $\ell$ values for the observed $\Delta\theta_i$'s, and the number of MC sets having $\ell$ values less than that of the observed sample is counted. The result is expressed in (absolute) probability in Table III. We can see that most models are not rejected and that only the no-selection-bias model is rejected if we include the large separation, non-single-galaxy lens cases, MG2016 and Q0957. Also, the model with the MG-C selection bias is rejected at $\sim 90\%$ level by the MG-C band survey samples.

### B. Kolmogorov-Smirnov Test

The MC simulation is quite versatile, being applicable even to the case where the distribution differs for each sample data. However, the test mainly focuses on whether the data occur at the probable part of the distribution. It does not test whether the data are clustered or not. The KS test is complementary to the MC simulation because it has good discriminative power on the clustering of the data. Hence, we use the KS two-sided test to find out if the calculated distribution is significantly different from that of the observed samples. This is possible because in a flat universe the distribution of separation angles is the same regardless of the source redshift, thus making the KS test easily applicable.

The CDF's constructed from the observed lens samples (*jagged lines*) and from the calculated distribution (*smooth curves*) are shown in Fig. 2: (a) the *dot-dashed* curve is CDF for no selection bias (NO), the *solid* line CDF from lens systems O-ALL, the *dotted* line from O-SINGLE, and the *dashed* line from O/R-SINGLE; (b) the *dotted* curve for bias HST and the *solid* line from corresponding lens systems; (c) the *dotted* curve for bias PSF1.0, the *short-dashed* curve for bias PSF0.7, the *long-dashed* curve for bias EYE1.0, the *dot-dashed* curve for bias EYE0.7 and the *solid* line from corresponding lens systems; (d) the *dotted* curve for bias MG-C and the *solid* line from corresponding lens systems. The comparisons between the observed and the calculated CDF's show the largest differences for the NO bias and the MG-C bias models.

The results of the KS test applied to each bias case are shown in Table IV. The numbers show the confidence of rejection, and only NO-O-ALL and MG-C are rejected with more than 95% confidence. This is in agreement with the MC test results. Hence, we can say that *although the observed optical lens systems show somewhat different distribution from theoretical ones, the difference is not statistically significant*. Only the radio lens systems show statistically significant inconsistencies with the "standard" lens statistics calculation. However, this is based on only four systems. If we dismiss lens system MG2016 which has two lensing galaxies, the sample consists of only three systems. Hence, although a statistically significant conclusion can be drawn formally, it is based on a few lens systems and should be taken with cautions.

### C. Without the $(3/2)^{1/2}$ Factor

Turner et al. [1] were the first to introduce the correction factor $(3/2)^{1/2}$ to convert the observed velocity dispersion (of luminous matter) into that of dark matter for E and S0 galaxies (also see Ref. [7]). However, Kochanek argues against this correction [2] and estimates a "90% confidence range" in the velocity dispersion which is significantly smaller than the $(3/2)^{1/2}$ corrected value. Hence, we repeat the calculation and the test without the $(3/2)^{1/2}$ factor. Since the image separation in a SIS lens is directly proportional to the square of the velocity dispersion, the mean image separation get smaller by 67% and the whole distribution moves to smaller values. The PDF's with and without the $(3/2)^{1/2}$ factor are compared in Fig. 3 (*solid* for with and *dotted* for without). The result of the MC test is summarized in Table III: All models, except HST and EYE1.0, have probabilities less than 10%, and the no-selection-bias models and MG-C model have probabilities less than 5%. The result of the KS test is shown in Table IV: Again, the confidence of rejection is $\gtrsim 90\%$ for all models except HST, and no-selection-bias models and the MG-C model are rejected by the observed lens systems with more than 97% confidence. To summarize, if the $(3/2)^{1/2}$ factor is really unnecessary, the observed lens data reject the "standard" lens statistics models, marginally or strongly depending on the angular selection biases and the corresponding data sets used.

## V. DISCUSSION

There are several factors which can contribute to the uncertainties in the probability distribution and in the statistical test. Firstly, the test depends sensitively on the observation sample due to the small number of appropriate lensing cases. From the analysis, we have seen that the conclusion does depend on which observed lens systems are chosen. This problem will disappear when we have enough lens systems.

We may increase the observed sample size by including other lens systems like Q0957+561 where the lensing galaxy is aided by a cluster. However, then the theoretical calculation should be modified accordingly to incorporate such multiple deflector cases. We think it is misleading to include lens system like Q0957 in the observed sample and to compare it with the theoretical distribution calculated by assuming only one galaxy as the deflector. However, this was done in many previous works [8,11,12,2].

It is also possible to use the measured redshifts of the deflectors and to calculate the distribution of image separations for a given lens redshift and source redshift. This approach would be useful if we had enough lens systems because the distribution in this case would depend on $\Omega_0$ and $\lambda_0$ individually and would be relatively insensitive to magnification bias. However, the number of lens systems found so far is too small to make any statistically significant discrimination [13]. We need more clean lens cases to make the test meaningful.

Secondly, the presence of cores in the galaxies and asphericity certainly affects the distribution. The core radii of galaxies are generally small enough to make SIS a good approximation [1,11]. If the core radii are not smaller than the typical image separations in the lens plane, the expected separation of images will be smaller and the discrepancy will be larger. The ellipticity can affect lensing frequencies via the magnification bias [14,2]. However, the distribution of image separations is relatively insensitive to the magnification

bias— the magnification bias can affect the distribution only indirectly through the angular selection bias which is weakly linked to the magnification bias [12]. It is possible to have high magnification events having much smaller separations than the characteristic values of the SIS cases. However, these types of events are expected to be rare [7].

The rather strong disagreement between the observation and the theoretical expectation, when we omit the $(3/2)^{1/2}$ factor, is not apparent in the extensive maximum likelihood study of Kochanek [2]. The main reason for this difference is the observed lens systems used. Lens systems Q1208+101, B1938+666, and B0218+356, all having $\lesssim 1''$ separations, are included in Kochanek's sample— they are omitted from our sample because they do not pass the criterion for the accepted case or because the image separation is not known yet.

Now, we can think of possible reasons for the discrepancy between the probability distribution from the theory and that from the observational data. The main ingredients of the "standard" model can be divided into two parts: one regarding cosmology and the other regarding galaxies. To determine if different cosmological model would change the test result, we tried two non-flat cosmological models (the open model with $\Omega_0 = 0.1$, $\lambda_0 = 0$ and the closed model with $\Omega_0 = 2$, $\lambda_0 = 0$). We applied a MC simulation test to these models. The probabilities from the MC simulations increased by $10 \sim 30\%$ for the closed universe and decreased by $20 \sim 30\%$ for the open universe because the image separation is smaller in an open universe and larger in a closed universe than in a flat universe [4]. Yet, the result was inconclusive again. Hence, the cause of the inconsistency between the "standard" model and the observation is likely to be in our poor understanding of galaxies rather than in the cosmological models. If this is the case, all previous works using the "standard" lensing statistics model to probe the cosmological parameters should be taken with caution.

## VI. SUMMARY

We calculated the distribution of image separations in the "standard" gravitational lens statistics model where the universe is flat and lensing galaxies are modeled by SIS's which follow the Schechter luminosity function and whose comoving density is kept constant. The calculated distribution of image separations, incorporating the angular selection bias, is compared, through the MC and the KS tests, with that seen in the observed lens systems.

The calculated distribution implies that a significant fraction of observed single-galaxy lens systems should have image separations $\lesssim 1''$, whereas most of the observed lens systems have separations larger than $1''$. However, the distribution is wide enough that the observations do not reject the "standard" lensing statistics model with enough statistical significance. The model without consideration of the angular selection bias is nearly ruled out, and the radio data strongly rules out the "standard" model. However, this conclusion, although statistically significant, is based on only four or three lens cases.

If the correction factor $(3/2)^{1/2}$—for converting the observed velocity dispersion to that of dark matter— is not used in the lens statistics calculations, the "standard" model is mostly rejected by the observations, although the ground-based survey is marginally compatible with the "standard" model. Also, larger core radii produce smaller image separations, and the discrepancy between the "standard" model and the observation will be greater, though the core radii of most galaxies are thought to be small enough to make SIS a good approximation.

The greatest difficulty in this or similar work is the small number of observed lens systems suitable for this kind of statistical analysis. We need to have more “clean” lens cases, meaning a single galaxy acting as lens. We hope that projects like Sloan Digital Sky Survey will answer most of the problems we have now.


## ACKNOWLEDGMENTS

We thank the referee for useful comments. This work was supported in part by Korea Research Foundation and in part by Korean Science and Engineering Foundation.

# REFERENCES


[1] E. L. Turner, J. P. Ostriker, and J. R. Gott, Astrophy. J. **284**, 1 (1984).

[2] C. S. Kochanek, Astrophy. J. **419**, 12 (1993).

[3] S. Refsdal, Mon. Not. Roy. Ast. Soc. **128**, 295 (1964); W. H. Press and J. E. Gunn, Astrophy. J. **185**, 397 (1973).

[4] J. R. Gott, M-G. Park, and H. M. Lee, Astrophys. J. **338**, 1 (1989).

[5] E. L. Turner, Astrophys. J. Lett. **365**, L43 (1990).

[6] M. Fukugita, T. Futamase, and M. Kasai, Mon. Not. Roy. Ast. Soc. **246**, 25 (1990).

[7] M. Fukugita and E. L. Turner, Mon. Not. Roy. Ast. Soc. **253**, 99 (1991).

[8] M. Fukugita, T. Futamase, M. Kasai, and E. L. Turner, Astrophy. J. **393**, 3 (1992).

[9] S. M. Faber and R. E. Jackson, Astrophys. J. **204**, 668 (1976); R. B. Tully and J. R. Fisher, Astron. Astrophys. **54**, 661 (1977).

[10] G. Efstathiou, R. S. Ellis, and B. A. Peterson, Mon. Not. Roy. Ast. Soc. **232**, 431 (1988)

[11] D. Maoz and H-W. Rix, Astrophy. J. **416**, 425 (1993).

[12] C. S. Kochanek, Astrophy. J. **417**, 438 (1993).

[13] H. Lee and M-G. Park, J. Kor. Ast. Soc. **27**, 103 (1994).

[14] S. Wallington and R. Narayan, Astrophy. J. **403**, 517 (1993).

[15] B. F. Burke, J. Lehàr, and S. R. Connor, *Gravitational Lenses*, edited by R. Kayser, T. Schramm, and L. Nieser (Springer, Berlin, 1992).

[16] S. Surdej and G. Soucail, *Proceedings of the 31st Liège International Astrophysical Colloquium*, "Gravitational Lenses in the Universe," edited by J. Surdej, D. Fraipont-Caro, E. Gosset, S. Refsdal, and M. Remy (Univ. de Liège, Belgium, 1993) and its updated version of the List of Gravitatinal Lens Systems (1995).

## FIGURES

FIG. 1. Probability distribution functions of image separations in multiple-image lens systems for various angular resolution biases: NO (*solid line*), HST (*dotted line*), PSF1.0 (*short dashed line*), PSF0.7 (*long dashed line*), EYE1.0 (*short dash-dotted line*), EYE0.7 (*long dash-dotted line*), and MG-C (*long dash-short dashed line*). Larger triangles mark the image separations in the lens systems PG1115, Q2237, Q0142, H1413, MG0414, and B1422. Smaller triangles mark those in Q1208 and MG2016.

FIG. 2. Cumulative distribution functions (CDF's)—fraction of cases with separations smaller than $\Delta\theta$— for various resolution biases and those from observed lens cases: (a) the *dot-dashed* curve is CDF for no selection bias (NO), the *solid* line CDF from lens systems O-ALL, the *dotted* line from O-SINGLE, and the *dashed* line from O/R-SINGLE; (b) the *dotted* curve for bias HST and the *solid* line from corresponding lens systems; (c) the *dotted* curve for bias PSF1.0, the *short-dashed* curve for bias PSF0.7, the *long-dashed* curve for bias EYE1.0, the *dot-dashed* curve for bias EYE0.7, and the *solid* line from corresponding lens systems; (d) the *dotted* curve for bias MG-C and the *solid* line from corresponding lens systems.

FIG. 3. PDF's with [*solid*] and without [*dotted*] the $(3/2)^{1/2}$ correction factor for no selection bias (a) and for MG-C selection bias (b).

# TABLES

TABLE I. Relevant multiple image gravitational lens systems.

| Lens system | $\Delta\theta$[a] | $z_S$ |
|---|---|---|
| PG1115[b] | 2.3 | 1.72 |
| Q2237[b] | 1.8 | 1.69 |
| Q0142[b] | 2.2 | 2.72 |
| H1413[b] | 1.1 | 2.55 |
| MG2016[c] | 3.8 | 3.27 |
| Q0957[d] | 6.1 | 1.41 |
| MG0414[e] | 3.0 | 2.64 |
| B1422[e] | 1.3 | 3.62 |
| Q1208[f] | .47 | 3.80 |
| MG1131[g] | 2.1 | 1.13? |
| MG1654[g] | 2.1 | 1.74 |

[a]Maximum image separation.

[b]Discovered in an optical observation. Lensed by a single galaxy.

[c]Discovered in an optical observation. Lensed by two galaxies.

[d]Discovered in an optical observation. Lensed by a galaxy plus cluster.

[e]Discovered in a radio observation. Lensed by a galaxy.

[f]Classified as a proposed case [16].

[g]Radio ring.

TABLE II. Angular selection bias and corresponding lens systems.

| Selection Bias | Lens Systems |
|---|---|
| NO[a] | 1115, 2237, 0142, 1413, 2016, 0957 (O-ALL[b]) |
| NO[a] | 1115, 2237, 0142, 1413 (O-SINGLE[c]) |
| NO[a] | 1115, 2237, 0142, 1413, 0414, 1422 (O/R-SINGLE[d]) |
| HST[e] | 1115, 2237, 0142, 1413, 1208 |
| PSF1.0[f] | 1115, 2237, 0142, 1413 |
| PSF0.7[g] | 1115, 2237, 0142, 1413 |
| EYE1.0[h] | 1115, 2237, 0142, 1413 |
| PSF0.7[i] | 1115, 2237, 0142, 1413 |
| MG-C[j] | 2016, 0414, 1131, 1654 |

[a]No selection bias.

[b]Lens systems discovered in optical observations.

[c]Lens systems discovered in optical observations. Lensed by a single galaxy or lens not known.

[d]Lens systems discovered in optical or radio observations. Lensed by a single galaxy or lens not known.

[e]Selection bias for the HST snapshot survey.

[f]Selection bias for ground-based optical observations with the PSF subtraction method and a seeing FWHM=1.0" [12].

[g]Selection bias for ground-based optical observations with the PSF subtraction method and a seeing FWHM=0.7" [12].

[h]Selection bias for ground-based optical observations with visual examination and a seeing FWHM=1.0" [12].

[i]Selection bias for ground-based optical observations with visual examination and a seeing FWHM=0.7" [12].

[j]MG C band survey [15,2]

TABLE III. Monte-Carlo simulation results.

| Selection Bias/Samples | Probability[a] | |
|---|---|---|
| | With $(3/2)^{1/2}$ | Without $(3/2)^{1/2}$ |
| NO-O-ALL | .01 | .00 |
| NO-O-SINGLE | .37 | .04 |
| NO-O/R-SINGLE | .30 | .01 |
| HST | .56 | .11 |
| PSF1.0 | .47 | .08 |
| PSF0.7 | .42 | .06 |
| EYE1.0 | .52 | .12 |
| EYE0.7 | .44 | .07 |
| MG-C | .09 | .00 |

[a]Fraction of MC draws having likelihood smaller than that of the observed data.

TABLE IV. Kolmogorov-Smirnov test results.

| Selection Bias/Samples | Confidence of Rejection[a] | |
|---|---|---|
| | With $(3/2)^{1/2}$ | Without $(3/2)^{1/2}$ |
| NO-O-ALL | .94 | .998 |
| NO-O-SINGLE | .71 | .97 |
| NO-O/R-SINGLE | .87 | .995 |
| HST | .17 | .81 |
| PSF1.0 | .53 | .92 |
| PSF0.7 | .60 | .94 |
| EYE1.0 | .39 | .89 |
| EYE0.7 | .50 | .92 |
| MG-C | .98 | .999 |

[a]Confidence to reject the null hypothesis that data come from the model distribution.

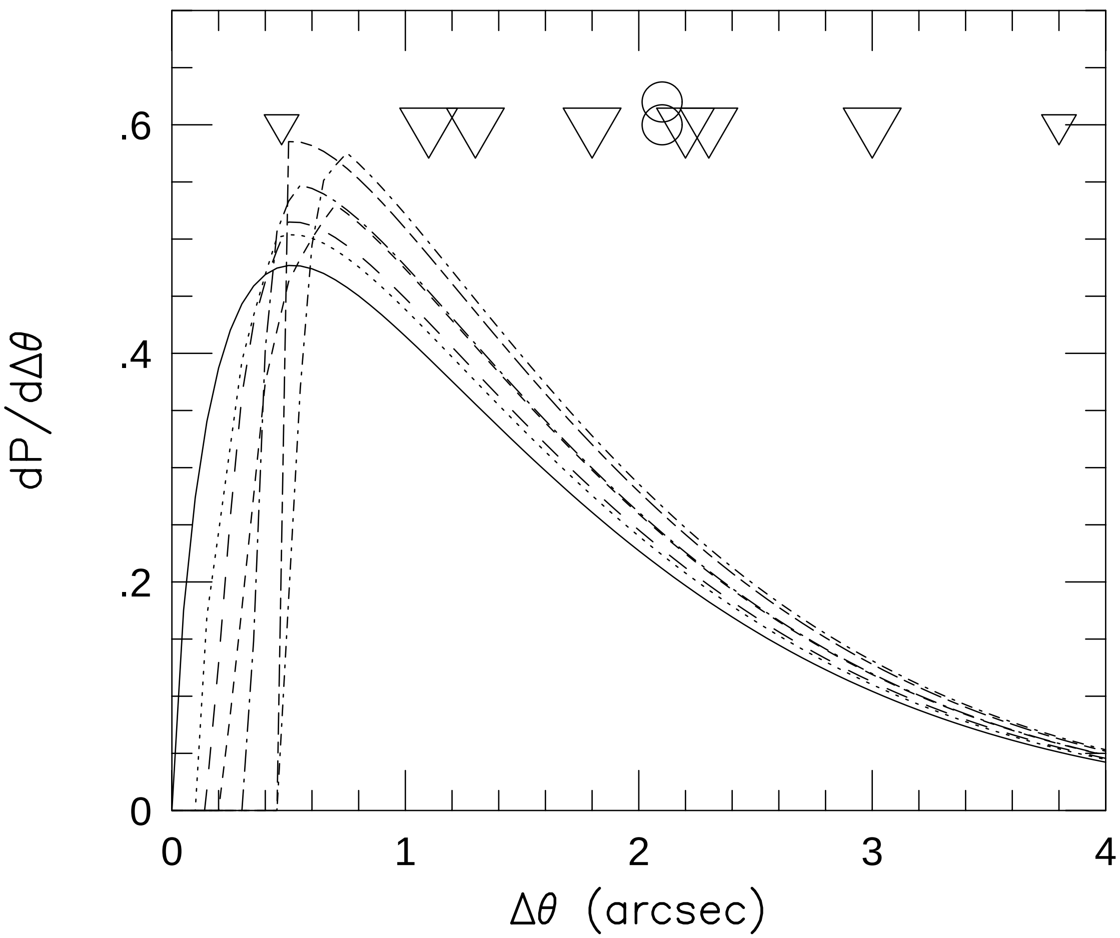

dP/dΔθ
.6
.4
.2
0
0
1
2
3
4
Δθ (arcsec)

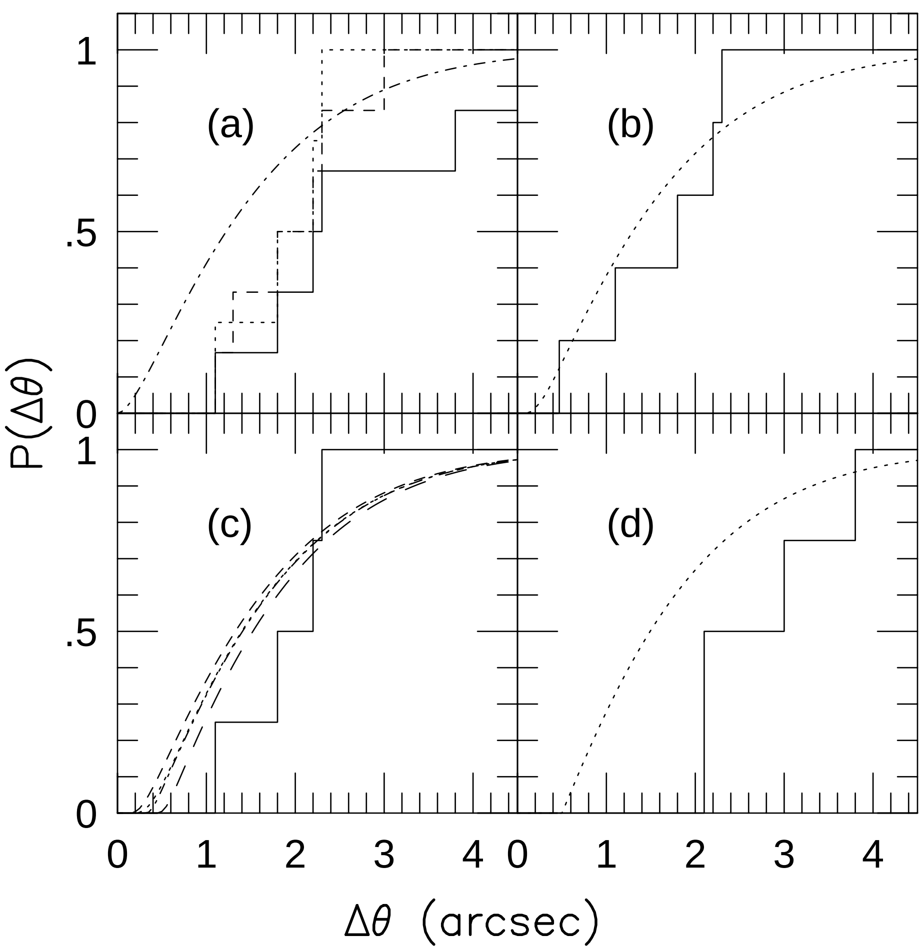

(a)
(b)
(c)
(d)
P(Δθ)
Δθ (arcsec)
0
.5
1
0
.5
1
0
1
2
3
4
0
1
2
3
4

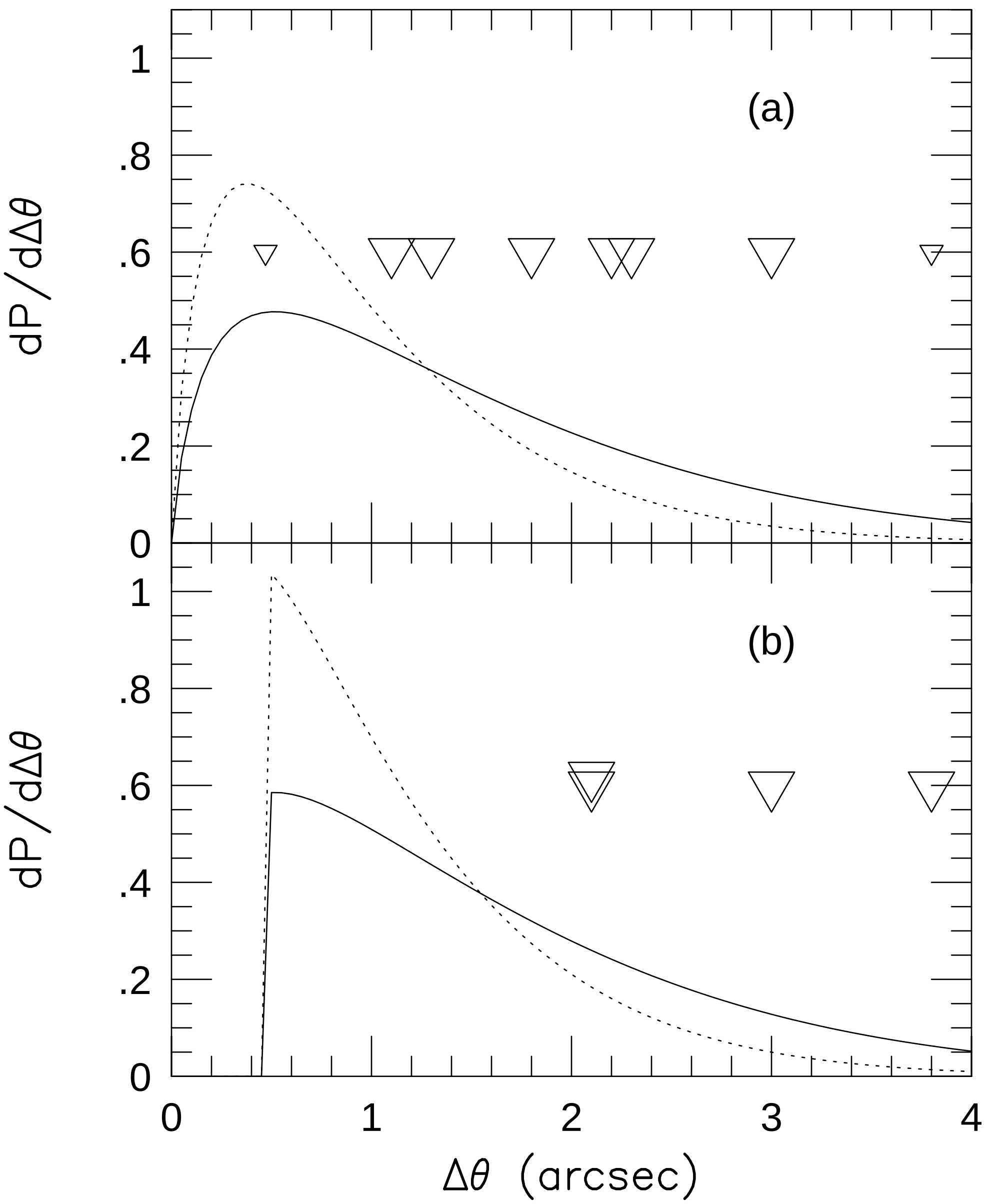
(a)
(b)
dP/dΔθ
dP/dΔθ
0
.2
.4
.6
.8
1
0
.2
.4
.6
.8
1
0
1
2
3
4
Δθ (arcsec)